Quantum Hall ferroelectrics and nematics in multivalley systems

Inti Sodemann,[1] Zheng Zhu,[1] and Liang Fu[1]

[1]*Department of Physics, Massachusetts Institute of Technology, Cambridge, Massachusetts 02139, USA*

(Dated: January 30, 2017)

We study broken symmetry states at integer Landau level fillings in multivalley quantum Hall systems whose low energy dispersions are anisotropic. When the Fermi surface of individual pockets lacks twofold rotational symmetry, like in Bismuth (111) surfaces [1], interactions tend to drive the formation of quantum Hall ferroelectric states. We demonstrate that the dipole moment in these states has an intimate relation to the Fermi surface geometry of the parent metal. In quantum Hall nematic states, like those arising in AlAs quantum wells, we demonstrate the existence of unusually robust skyrmion quasiparticles.

arXiv:1701.07836v1 [cond-mat.str-el] 26 Jan 2017

Introduction—Quantum Hall liquids with nearly degenerate internal degrees of freedom have long been the source of a rich variety of phenomena. Aside from multilayer systems, there exist today an array of multi-valley two-dimensional electron systems exhibiting quantum Hall effect, including AlAs heterostructures [2], monolayer and bilayer graphene [4, 5], Si surfaces [6], PbTe (111) quantum wells [7], surface states of the topological crystalline insulator $Sn_{1-x}Pb_xSe$ [8], and more recently the (111) surface of Bismuth [1]. These systems all have multiple valleys centered at different regions in momentum space, which are related to each other by the rotational symmetry of the crystal.

Among these multivalley systems, AlAs heterostructures, Si surfaces, PbTe (111) quantum wells and Bi(111) surfaces all have highly anisotropic pockets, whose orientations are valley-dependent. The shape of Fermi surface, which is determined by the electronic band structure of the host material, is crucial in determining the pattern of valley symmetry breaking. For AlAs, and PbTe, the pockets are centered at time-reversal-invariant momenta, and therefore each pocket has an elliptical shape with two-fold symmetry. This twofold Fermi surface anisotropy favors a valley-polarized quantum Hall state where a subset of valley degenerate Landau levels are fully occupied [2, 10]. This state spontaneously breaks the larger crystal rotational symmetry into a twofold one and is thus a nematic quantum Hall state.

However, the recently studied Bi(111) surface and $Sn_{1-x}Pb_xSe$ (001) surface, brings in a novel ingredient into this problem. As shown in (Fig. 1), Bi (111) surface has six tadpole-shaped hole pockets [11]; $Sn_{1-x}Pb_xSe$ (001) surface has four crescent-shaped pockets [12]. These pockets come in time-reversed pairs located at opposite momenta away from time-reversal-invariant points in the Brillouin zone. Importantly, Fermi surface of each pocket does *not* have a twofold rotational symmetry. Therefore, we expect Landau orbitals associated with each valley generically to carry an in-plane electric dipole moment. This implies that a valley-polarized state can possess an electric polarization, rendering the resulting quantum Hall state a ferroelectric. The giant fermi surface anisotropy of Bi(111) and $Sn_{1-x}Pb_xSe$ (001) surface states makes them promising candidate systems to study this novel ferroelectricity in quantum Hall states (Fig. 1).

In this letter we provide a unified description of these ferroelectric and nematic states in multi-valley integer quantum Hall systems. We establish that due to Fermi surface anisotropy, the long-range Coulomb interaction generically favors states with full valley polarization. We compute the electric polarization of quantum Hall ferroelectrics using a quantum mechanical approach based on Berry phase and also using a semiclassical approach that directly relates the dipole moment to the underlying Fermi surface geometry. For quantum Hall nematic states, we study the energetics of Skyrmion-type charged excitations [13] using the density-matrix renormalization group method, and find they are suprisingly robust against mass anisotropy of the valleys, shedding new insights on the experiments on AlAs quantum wells [14].

General setup—We start from symmetry considerations on two-dimensional (2D) multivalley systems. We consider systems with three, four, or six fold rotational symmetry, which rules out any principal axis within the 2D plane. In order for each valley to have an anisotropic dispersion, we require that the symmetry group that leaves each valley invariant, or the "little group", is only a subgroup of C_{2v}, or equivalently, contains no more than a twofold rotation $(x, y) \rightarrow (-x, -y)$ and at most two mirror planes that are orthogonal to each other, $(x, y) \rightarrow (-x, y)$ and $(x, y) \rightarrow (x, -y)$.

There are two types of systems with multiple anisotropic valleys: type-I are those whose little group contains at most a single mirror plane; type-II are those with larger symmetry. For systems of the first type, each valley is of such low symmetry that the electron dispersion at zero field has no inversion center, i.e., $\epsilon(\mathbf{k}) \neq \epsilon(-\mathbf{k})$ where $\mathbf{k}$ is the "small" momentum within the valley. As we will show, in the quantum Hall regime and at odd-integer fillings, Coulomb interaction induces a valley-polarized state which breaks all rotational symmetry of the crystal and is therefore a ferroelectric. For systems of the second type, the electron dispersions at each valley have twofold symmetry $\epsilon(\mathbf{k}) = \epsilon(-\mathbf{k})$. In this case, valley-polarized quantum Hall states exhibit nematic instead of ferroelectric orders. The Bi(111) surface [1] is a representative of type-I systems and the AlAs (001) quantum well [2] a representative of type-II.

To study interacting electrons in multi-valley quantum Hall systems we assume that the magnetic field is large enough so that the Hamiltonian can be projected into a set of M nearly degenerate Landau levels levels associated with different valleys. The system is at some partial integer filling $\nu \in \mathbb{Z}$ ($\nu \leq M$). The interaction between an electron with position $\mathbf{r}_1$ from valley i and an electron with position $\mathbf{r}_2$ from valley j is dominated by the *long-range* part of the Coulomb inter-

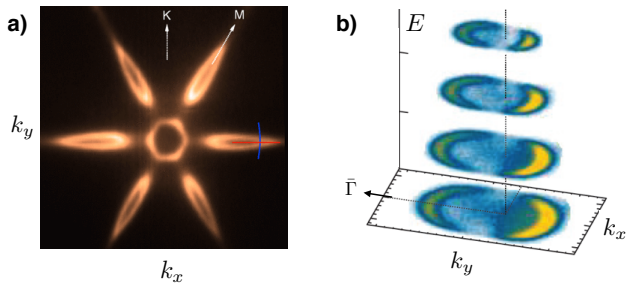

FIG. 1: (color online) Measured ARPES fermi surfaces of a) Bi(111) surface from Ref 11 and b) $Sn_{1-x}Pb_xSe$ (001) surface from Ref 12.

action, which depends only on their distance $|\mathbf{r}_1 - \mathbf{r}_2|$, i.e., $v(\mathbf{r}_1 - \mathbf{r}_2) = 1/A \sum_{\mathbf{q}} v_{\mathbf{q}} e^{i\mathbf{q}\cdot(\mathbf{r}_1-\mathbf{r}_2)}$ [35]. Note that v is independent of the relative orientation of the two electrons, because systems considered here all have isotropic dielectric properties. Despite the bare Coulomb interaction being valley independent, it becomes valley dependent after projection into the Landau levels:

$$P_0 v(\mathbf{r}_1 - \mathbf{r}_2) P_0 = \frac{1}{A} \sum_{\mathbf{q}} v_{\mathbf{q}} F_i(\mathbf{q}) F_j(-\mathbf{q}) e^{i\mathbf{q}\cdot(\mathbf{R}_1-\mathbf{R}_2)}, \quad (1)$$

where $\mathbf{R} \equiv \mathbf{r} - l^2 \hat{\mathbf{z}} \times \mathbf{p}$ is the intra-Landau level guiding center operator, $\mathbf{p} = \nabla/i - e\mathbf{A}$ is the mechanical momentum, and $F_i(\mathbf{q}) \equiv \langle i, n | e^{-il^2 \hat{\mathbf{z}}\cdot\mathbf{q}\times\mathbf{p}} | i, n \rangle$ is the form factor determined by the wavefunction, $|i, n\rangle$, of the Landau level of interest associated with valley i ($\hbar \equiv 1$, $l^2 \equiv 1/eB$). These form factors are crucial for the energetics of valley symmetry breaking quantum Hall states and are described in detail for type-I and type-II multi-valley systems in the Supplementary material [34].

We study the Hamiltonian (S10) using both Hartree-Fock approximation and DMRG numerical method. Within Hartree-Fock, we consider translationally invariant trial Slater determinant states that are arbitrary coherent superpositions of the M valleys. Their energy (including the neutralizing background) can be found to be:

$$\begin{aligned} E[P] &= -N_\phi \sum_{i,j} X_{ij} \langle i|P|j\rangle\langle j|P|i\rangle, \\ P &= \sum_{a=1}^{\nu} |\chi_a\rangle\langle\chi_a|, \; X_{ij} = \frac{1}{2} \int \frac{d^2\mathbf{q}}{(2\pi)^2} v_{\mathbf{q}} F_i(\mathbf{q}) F_j^*(\mathbf{q}). \end{aligned} \quad (2)$$

where i labels the valleys and $|\chi_a\rangle$ are ν orthonormal vectors describing the occupied coherent combinations of the valleys. Trial states are found by minimizing $E[P]$ as a function of P.

At $\nu = 1$ the state that minimizes the Hartree-Fock energy is maximally polarized into a single valley under very general conditions. In fact we prove the following *theorem*: if the set of form factors $F_i(\mathbf{q})$ with $i = 1, ..., \nu$ are linearly independent functions of $\mathbf{q}$ and the interaction is strictly positive $v_{\mathbf{q}} > 0$, the minimum of $E[P]$ at $\nu = 1$ for a system with multiple anisotropic valleys is a state maximally polarized into a single valley. The proof is provided in the supplementary material [34]. To check that form factors are linearly independent one simply needs to show that $\det(X_{ij}) \neq 0$.

Form factors are generically linearly independent for valleys with anisotropic Fermi surfaces that are *distinct*. We use the word *distinct* here in a strong sense. For example, two elliptical Fermi surfaces that are rotated with respect to each other, as in AlAs, are *distinct*. Similarly, all the Fermi surfaces at the Bi(111) surface are *distinct* (Fig. 1). Therefore, we expect generically that the ground states of type-I and type-II systems is a fully valley polarized ferroelectric or nematic state at $\nu = 1$.

It is possible, however, that two Fermi surfaces for distinct valleys are, in a small momentum approximation, identical (as in the case of graphene within the Dirac approximation), hence the form factors are linearly dependent. These system in the presence of long-range Coulomb interaction have an emergent SU(2) symmetry. Also, an important condition for the above theorem on multicomponent quantum Hall states is that all electrons reside in the same layer so that the interactions before projecting to the Landau level are identical. Otherwise, non-trivial Hartree terms may favor superpositions of components in different layers, as it happens for the exciton condensate in quantum Hall bilayers [32].

Our Hartree-Fock analysis is confirmed by our momentum-space DMRG [16–20] simulations on the torus geometry. This is implemented by mapping the single particle orbitals in the Landau gauge into a one dimensional chain. Details can be found in Supplementary Material [34].

Quantum Hall ferroelectrics—In this section we consider multi-valley systems of the type-I, where anisotropic valleys are located at non-time-reversal-invariant momenta and each valley lacks twofold symmetry. This type of multi-valley systems is realized on the (111) surface of bismuth [11], and on the (001) surface of topological crystalline insulators SnTe, $Sn_xPb_{1-x}Se$ and $Sn_xPb_{1-x}Te$ [21]. In both materials, surface state Landau levels have been observed by scanning tunneling microscopy [1, 8].

Type-I systems exhibit a fully valley polarized state at total filling $\nu = 1$ [34] that fully breaks rotational symmetry. Because the quantum Hall state is insulating in the bulk, we expect a spontaneous electric polarization to develop, whose magnitude can be computed by adapting the modern theory of polarization based on Berry phase [5]. We find the dipole moment per electron along the y direction is given by:

$$D_y = -i|e| \frac{l^2}{L_x} \int_0^{L_x/l^2} dk_y \langle u_{k_y} | \partial_{k_y} | u_{k_y} \rangle. \quad (3)$$

where $|u_{k_y}\rangle$ are single particle orbitals in a gauge that is translationally invariant along y for the Landau level of interest [34]. An analogous expression holds for the dipole along the x axis. Alternatively, the dipole can also be obtained by computing the displacement of the average position of each occupied single particle state. Both calculations agree, as demonstrated in [34].

We now introduce a semiclassical approach to establish a direct connection of the dipole moment with the underlying

Fermi surface geometry at zero field. Consider a valley described by a single-band Hamiltonian $H(\mathbf{p})$ of arbitrary form. By choosing the Landau gauge $A_x = 0$ and $A_y = Bx$, we can view the eigenvalue problem as effectively one-dimensional. Writing the wavefunction as $\psi_{k_y}(x, y) = u_{k_y}(x)e^{ik_y y}/\sqrt{L_y}$, we have:

$$H\left(\frac{\hbar}{i}\frac{d}{dx}, k_y - eBx\right)u_{k_y}(x) = \epsilon_n u_{k_y}(x). \tag{4}$$

We set $k_y = 0$ (other solutions are obtained by a global translation). The WKB method leads to an approximate wavefunction of the form:

$$u_0(x) \approx \sum_s \frac{1}{\sqrt{v^{\rm cl}_{x,s}(x, \epsilon_n)}} \exp\left(\frac{i}{\hbar}\int^x dx' p^{\rm cl}_{x,s}(x', \epsilon_n)\right), \tag{5}$$

where $p^{\rm cl}_{x,s}(x', \epsilon_n)$ is the s root of the classical energy relation: $H(p^{\rm cl}_{x,s}, -eBx) = \epsilon_n$, and $v^{\rm cl}_{x,s}(x, \epsilon_n) = \partial H(p_x, -eBx)/\partial p_x$. Typically we have two roots $s = +, -$ and two turning points $x_{+,-}$ that separate the classically allowed region from the classically forbidden region. Matching boundary conditions between classically allowed and forbidden regions leads to the Onsager quantization condition: $l^2 A(\epsilon_n) = 2\pi(n + 1/2)$, where $A(\epsilon_n)$ is the area in momentum space inside the isoenergetic contour $H(\mathbf{k}) = \epsilon_n$ and n is the Landau level index. From Eq. (S46) the dipole can be written as $D_y = -el^2 \int dx\, \mathrm{Im}(u_0^*(x)\partial_x u_0(x))$. In the semiclassical limit of large n this expression reduces to a simple form [34] and one finds that dipole moment is given by time averaged position of the electron over the semiclassical orbit:

$$\mathbf{D} \approx -|e|\langle \mathbf{r}(t, \epsilon_n)\rangle_t \equiv -|e|\frac{\oint dt\, \mathbf{r}(t, \epsilon_n)}{\oint dt}, \tag{6}$$

where the integral is perfomed over the semiclassical cyclotron orbit $\mathbf{r}(t) = l^2\mathbf{k}(t) \times \hat{z}$, with $\mathbf{k}(t)$ tracing a constant energy contour $H(\mathbf{k}(t)) = \epsilon_n$ at a speed $v = |\partial\epsilon/\partial\mathbf{k}|$ [6]. This picture predicts intuitively and generically that the dipole is orthogonal to the direction of the distortion of the Fermi surface since the real space orbit is a rotated version of the Fermi surface [34].

The above semiclassical approach is applicable to high Landau levels $n \gg 1$ such as those observed in Bi (111) surface. To study ferroelectricity in $n \sim 1$ Landau levels, we consider a model with two valleys ($M = 2$) of Dirac fermions located at opposite momenta, at filling $\nu = 1$. This model describes the low-energy dispersion of the [001] surface of SnTe and Pb-SnTe topological crystalline insulators in the low temperature phase [22]. Here, the Dirac cones are generically "tilted" [7] and described by the following Hamiltonian:

$$H_0 = \pm v_x\sigma_x p_x + v_y\sigma_y p_x \pm \delta v_x p_x, \tag{7}$$

The only discrete symmetry that leaves each valley invariant is a single mirror plane along the line that connects the Dirac cones [7, 22]. We consider the $n = 1$ Landau level [36]. The wavefunctions associated with each valley break rotation and inversion symmetry as illustrated in Fig. 2. The Hartree-Fock energy is (up to a global constant) $E/A = -\beta n_z^2$, where $n_z = \mathrm{tr}(\sigma_z P)$ and σ_z is a Pauli matrix in the valley indices, and β is positive [34], in agreement with our theorem of full valley polarization. Therefore, the ground state is of Ising type ($n_z = \pm 1$) with coexisting ferroelectric and nematic properties. The dipole moment, to leading order in the Dirac cone tilt, can be found to be:

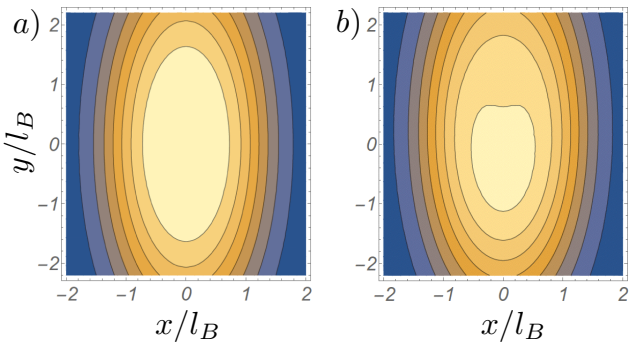

FIG. 2: (color online) Probability amplitude contours for coherent states in the first Landau level of a Dirac cone with anisotropic velocities $v_x/v_y \approx 2.2$ (a), and with anisotropy and tilt $\delta v_x \approx 0.3$ (b). The wavefunction carries a dipole moment perpendicular to the tilt of the Dirac cone.

$$D_y \approx \mp|el|\mathrm{sign}(B)\frac{\delta v_x}{\sqrt{v_x v_y}}\left(1 - \frac{1}{2\sqrt{2}}\right),\ D_x = 0. \tag{8}$$

As expected the dipole of a given valley is orthogonal to the direction of the Dirac cone tilt, and reverses with the direction of the perpendicular field. This is allowed because the magnetic field breaks the mirror symmetry present at zero field.

We now discuss potential experimental manifestations of the quantum Hall ferroelectric states on the Bi(111) surface [1], where we expect ferroelectric states to appear at odd integer fillings. One potential signature is the appearance of additional ferroelectric domain walls in addition to those associated with the nematicity seen at even fillings. Another interesting possibility is the existence of gapless conducting edge states at the ferroelectric domain walls. If one neglects inter-valley scattering, the valley pseudospin is conserved and one expects gapless charge carrying counter-propagating edge modes that arise at the domain walls [37]. Due to their ferroelectric nature, these domains may be manipulated by STM bias voltage or in-plane external electric field. Finally, we note that Bi (111) hole pockets located at opposite momenta carry opposite in-plane spin-polarizations, which cancel when the two are equally occupied. Therefore, valley-polarized quantum Hall states at odd-integer filling also carry an in-plane spin polarization, and thus can be manipulated by an in-plane magnetic field.

Valley skyrmions in quantum Hall nematics— In this section we consider multi-valley systems of type-II that de-

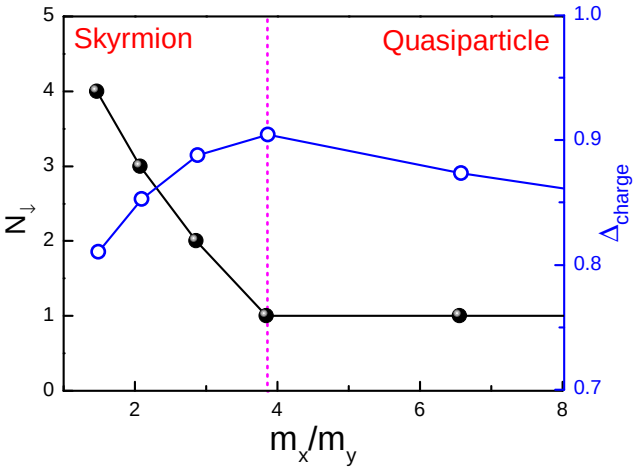

FIG. 3: (color online) Number of electrons in the minority valley (left vertical axis) for a quasiparticles as a function mass anisotropy ration in a two valley system (AlAs) and the charge gap (right vertical axis) computed with DMRG.

velop nematicity but which carry no dipole moment. We focus on the simplest non-trivial case with two valleys whose anisotropic mass tensors are rotated by a $\pi/2$ angle relative to each other. This is the scenario realized in AlAs systems [2, 2]. Other experimentally relevant scenarios along with useful formulae for their form factors are discussed in the supplementary material [34]. Our main objective is to study non-trivial charge excitations on these systems, but we briefly review ground state properties. At filling $\nu = 1$ one finds that the energy is (up to a global constant) $E/A = -\alpha n_z^2$, where $n_z = \mathrm{tr}(\sigma_z P)$, and $\alpha > 0$ [34]. The system has Ising character in agreement with our theorem of full valley polarization. The Ising nematic state is an exact eigenstate of the Hamiltonian projected into the valley degenerate Landau level. We confirmed that it is the ground state via DMRG approach employing a torus with a square aspect ratio $(1 : 1)$ [34] for as many as 24 electrons and for mass anisotropies as large as $m_x/m_y = 16$ [34].

Having established that the ground state is a nematic state, we now turn to study its charged excitations. In the SU(2) invariant limit, *i.e.* when the mass tensors are the same for both valleys, we expect the lowest energy excitation to be infinite sized skyrmions [13]. When the mass tensors are slightly different, we expect that the skyrmions will have a finite size dictated by the competition between the Ising anisotropy which wants to shrink them and the Coulomb energy which wants to expand them to smear the charge over large distances [38]. To be able to study accurately the properties of skyrmions we resort to DMRG [39]. The skyrmion quasi-electron can be obtained as the ground state of the Hamiltonian when $N = N_\phi + 1$ [40]. In Fig. 3 we show that non-trivial skyrmions (those involving at least one spin flip) survive up to large mass ratio $m_x/m_y \approx 3.8$ for the case of two valleys rotated by $\pi/2$ (as in AlAs). AlAs has a mass anisotropy of about $m_x/m_y \approx 5$ [2]. The experiment of Ref. [14] found a nonlinear dependence of the charge gap on strain, which was interpreted as evidence for skyrmions. Our findings suggest that this is scenario is not unlikely since the critical mass ratio to observe skyrmions is ultimately dependent on the details of interactions and can easily change by effects beyond our model (e.g. finite well widths and Landau level mixing).

In summary, we have shown that multivalley systems with anisotropic dispersions lead generically to ferroelectric or nematic quantum Hall states at odd integer Landau level fillings. The ferroelectric states arise when the parent Fermi surface of a single valley lacks an inversion center, such as the case of Bi(111) [1]. We have shown that the resulting dipole moment has an intimate relation with the underlying fermi surface geometry of the parent metal. We also demonstrated the existence of non-trivial skyrmion-type charged excitations in the nematic states with an unexpectedly large stability to the Ising symmetry breaking terms, shedding light into the question of the presence of these excitations in AlAs [14].

We would like to thank Vidya Madhavan, Benjamin Feldman, Malika Randeria, Ali Yazdani, Donna Sheng, Heun Mo Yoo, Joonho Jang and Ray Ashoori for stimulating discussions. I.S. is supported by the Pappalardo Fellowship. Z.Z. is supported by the David and Lucile Packard foundation. L.F. is supported by the DOE Office of Basic Energy Sciences, Division of Materials Sciences and Engineering under Award No. DE-SC0010526.

[1] B. E. Feldman, M. T. Randeria, A. Gyenis, F. Wu, H. Ji, R. J. Cava, A. H. MacDonald, and A. Yazdani, Science **354**, 316 (2016).
[2] M. Shayegan, E. P. De Poortere, O. Gunawan, Y. P. Shkolnikov, E. Tutuc, K. Vakili, Phys. Stat. Sol. b **243**, 3629 (2006).
[3] K. S. Novoselov, A. K. Geim, S. V. Morozov, D. Jiang, M. I. Katsnelson, I. V. Grigorieva, S. V. Dubonos, and A. A. Firsov, Nature **438**, 197 (2005).
[4] Y. Zhang, Y-W. Tan, H. L. Stormer, and P. Kim, Nature **438**, 201 (2005).
[5] K. S. Novoselov, E. McCann, S. V. Morozov, V. I. Fal'ko, M. I. Katsnelson, U. Zeitler, D. Jiang, F. Schedin, and A. K. Geim, Nature Physics **2**, 177 (2006).
[6] K. Eng, R. N. McFarland, and B. E. Kane, Phys. Rev. Lett. **99**, 016801 (2007).
[7] V. A. Chitta, W. Desrat, D. K. Maude, B. A. Piot, N. F. Oliveira Jr., P. H. O. Rappl, A. Y. Ueta, E. Abramof, Physica E: Low-dimensional Systems and Nanostructures **34**, 124 (2006).
[8] Yoshinori Okada, Maksym Serbyn, Hsin Lin, Daniel Walkup, Wenwen Zhou, Chetan Dhital, Madhab Neupane, Suyang Xu, Yung Jui Wang, R. Sankar, Fangcheng Chou, Arun Bansil, M. Zahid Hasan, Stephen D. Wilson, Liang Fu, Vidya Madhavan, Science 341, 6153 (2013)
[9] D. A. Abanin, S. A. Parameswaran, S. A. Kivelson, and S. L. Sondhi, Phys. Rev. B **82**, 035428 (2010); A. Kumar, S. A. Parameswaran, and S. L. Sondhi Phys. Rev. B **88**, 045133 (2013).

[10] X. Li, F. Zhang, A. H. MacDonald, Phys. Rev. Lett. **116**, 026803 (2016).
[11] Y. Ohtsubo, J. Mauchain, J. Faure, E. Papalazarou, M. Marsi, P. Le Fvre, F. Bertran, A. Taleb-Ibrahimi, and L. Perfetti, Phys. Rev. Lett. **109**, 226404 (2012).
[12] P. Dziawa, B. J. Kowalski, K. Dybko, R. Buczko, A. Szczerbakow, M. Szot, E. Lusakowska, T. Balasubramanian, B. M. Wojek, M. H. Berntsen, O. Tjernberg and T. Story, Nature Materials 11, 1023 (2012).
[13] S. L. Sondhi, A. Karlhede, S. A. Kivelson, and E. H. Rezayi, Phys. Rev. B **47**, 16419 (1993).
[14] Y. P. Shkolnikov, S. Misra, N. C. Bishop, E. P. De Poortere, and M. Shayegan, Phys. Rev. Lett. **95**, 066809 (2005).
[15] K. Moon, H. Mori, K. Yang, S. M. Girvin, A. H. MacDonald, L. Zheng, D. Yoshioka, and S-C. Zhang, Phys. Rev. B **51**, 5138 (1995).
[16] N. Shibata and D. Yoshioka, Phys. Rev. Lett. 86, 5755 (2001).
[17] A. E. Feiguin, E. Rezayi, C. Nayak, and S. Das Sarma, Phys. Rev. Lett. 100, 166803 (2008).
[18] T. Xiang, Phys. Rev. B 53, R10445 (1996).
[19] S. R. White, Phys. Rev. Lett. 69, 2863 (1992).
[20] J. Zhao, D. N. Sheng, and F. D. M. Haldane, Phys. Rev. B 83, 195135 (2011).
[21] Junwei Liu, Wenhui Duan, and Liang Fu, Phys. Rev. B 88, 241303 (2013).
[22] M. Serbyn and L. Fu, Phys. Rev. B **90**, 035402 (2014).
[23] I. Sodemann and L. Fu, Phys. Rev. Lett. **115**, 216806 (2015).
[24] D. J. Thouless, Phys. Rev. B **27**, 6083 (1983).
[25] R. D. King-Smith and D. Vanderbilt, Phys. Rev. B **47**, 1651(R) (1993).
[26] L. A. Falkovskii, J. Exptl. Theoret. Phys. (U.S.S.R.) **49**, 609 (1965); A. Yu. Ozerin and L. A. Falkovsky, Phys. Rev. B **85**, 205143 (2012).
[27] C. Kittel, Introduction to solid state, John Wiley & Sons, (1966).
[28] L. Onsager, Phil. Mag. **43**, 1006 (1952).
[29] D-W. Wang, E. Demler, and S. Das Sarma, Phys. Rev. B **68**, 165303 (2003).
[30] Y. Barlas, R. Ct, K. Nomura, and A. H. MacDonald, Phys. Rev. Lett. **101**, 097601 (2008).
[31] B. Yang, Z. Papić, E. H. Rezayi, R. N. Bhatt, and F. D. M. Haldane, Phys. Rev. B **85**, 165318 (2012).
[32] K. Moon, H. Mori, Kun Yang, S. M. Girvin, A. H. MacDonald, L. Zheng, D. Yoshioka, and Shou-Cheng Zhang, Phys. Rev. B 51, 5138 (1995).
[33] M. Abolfath, J. J. Palacios, H. A. Fertig, S. M. Girvin, and A. H. MacDonald, Phys. Rev. B **56**, 6795 (1997).
[34] Supplementary material.
[35] We neglect short distance valley dependent corrections.
[36] The zeroth Landau level does not carry dipole even in the presence of the tilt because the Hamiltonian retains an intra-valley particle-hole times inversion symmetry which forbids a dipole moment for the zeroth level. However, all other Landau levels will carry a dipole.
[37] We wish to note that other types of quantum Hall ferroelectrics arising in wide quantum wells [29] and in bilayer graphene [30] have been previously proposed, but to our knowledge these proposals have not been experimentally realized so far.
[38] The stiffness cost is scale invariant and hence indifferent to the size of the skyrmion.
[39] The energetics can be captured by a non-linear sigma model [13, 32], but using using long-wavelength estimates for non-linear sigma model parameters leads to a substantial underestimation the size of the skrymions [34]. This is a known pitfall of this type of estimates for small skyrmions [3].
[40] Quasi-hole and quasi-electron excitations are related by particle hole symmetry.

QUANTUM HALL FERROELECTRICS AND NEMATICS IN MULTIVALLEY SYSTEMS: SUPPLEMENTARY MATERIAL

Contents

I. Introduction 6

II. Landau levels and density form factors for anisotropic parabolic dispersions 6

III. Landau levels and density form factors for anisotropic Dirac cones 7

IV. Landau levels and density form factors in tilted Dirac cones 7

V. Hartree-Fock theory for multiple valleys 8
A. Two components at $\nu = 1$ 8
B. three-fold symmetric three-components at $\nu = 1$ 9
C. four-fold symmetric four-components at $\nu = 1$ 9

VI. Proof of full valley polarization for two anisotropic valleys at $\nu = 1$ within Hartree-Fock 9

VII. Proof of full valley polarization for multiple valleys at $\nu = 1$ within Hartree-Fock 10

VIII. Berry phase and position shift formulae of the electric Dipole moment in a Landau level 11

IX. WKB expression for the Dipole moment 12

X. Semiclassical picture of the cyclotron motion in tilted Dirac cones 13

XI. DMRG implementation 13

XII. Comparison between Hartree-Fock and DMRG quasiparticle gap 14

XIII. Ising skyrmions from non-linear sigma model 15

XIV. Simplified calculation of charge gap from particle-hole symmetry 16

References 17

I. INTRODUCTION

This supplementary material contains details of calculations presented in the main text but also extensions into a few other cases of interest. In Sections II to IV we derive wavefunctions and form factors for a variety of anisotropic systems and for different Landau levels. Section V explains the Hartree-Fock theory and presents the solutions of the Hartree-Fock minimization explicitly for the nematic case of valleys with elliptic Fermi surfaces that are related by discrete rotations. Sections VI and VII discuss the proof of the theorem of full valley polarization unifying the specific examples that are discussed in the main text and in Sec. V. Section VIII derives the Berry phase formula for the dipole using the modern theory of polarization and also shows that this formula is equivalent to the calculation based on the shift of the position of the electron measured from the guiding center. Section IX describes the WKB calculation of Landau level wavefunctions and their corresponding dipole moment in the semiclassical limit. Section X considers the semiclassical picture of the dipole for the case of the tilted Dirac cone. Section XI discussed the details of the DMRG implementation and the extrapolation of the gaps to thermodynamic limit along with the estimate of the skyrmion quasiparticle stability as a function of mass anisotropy. Comparison between the Hartree-Fock and DMRG charge gaps are discussed in Section XII illustrating the agreement of both approaches in the case of conventional quasiparticles and their significant deviation for skyrmions. Section XIII discusses the failure of a naive estimate for the stability of the skyrmions using bare long-wavelength parameters and a non-linear sigma model. And finally Sec. XIV shows a simplified way to compute the charge gap in the two component case of elliptic pockets using particle-hole symmetry and the knowledge of the energy of the quasi-electron.

II. LANDAU LEVELS AND DENSITY FORM FACTORS FOR ANISOTROPIC PARABOLIC DISPERSIONS

Consider the problem of Landau levels with an anisotropic mass tensor:

$$H = \frac{1}{2m^*} p_a g_{ab} p_b. \tag{S1}$$

Where $p = \nabla/i - eA$, and g is a tensor that can be diagonalized as $g = Q^T S^2 Q$, where $Q \in SO(2)$ and S is diagonal with positive eigenvalues and $\det S = 1$. We can define rescaled momenta along the principal axes of the tensor to be: $\pi_a = (SQ)_{ab} p_b$, these satisfy the same commutation relations as the original ones:

$$[\pi_a, \pi_b] = il^{-2}\epsilon_{ab}. \tag{S2}$$

Which allows to solve the LL problem by defining the LL raising operators:

$$a \equiv \frac{l}{\sqrt{2}}(\pi_x + i\pi_y), \tag{S3}$$

satisfying $[a, a^\dagger] = 1$. The guiding center operators are intra-Landau level operators defined as:

$$R_a \equiv r_a + l^2 \epsilon_{ab}\pi_b. \tag{S4}$$

They satisfy:

$$[R_a, R_b] = -il^2\epsilon_{ab},$$
$$[R_a, p_b] = [R_a, \pi_b] = 0. \tag{S5}$$

The single particle Hilbert space can be decomposed into a tensor product $|n\rangle\otimes|m\rangle$, where $|n\rangle$ are the Landau level indices on which $a, a^\dagger$ act and $|m\rangle$ are intra-Landau level indices on which R_a acts. Now the projected interaction into the Landau level of interest is obtained by imagining we have two flavors of particles with different mass tensors ($g_1 = Q_1^T S_1^2 Q_1$ and $g_2 = Q_2^T S_2^2 Q_2$) which interact via a potential that depends only on interparticle distance:

$$V(r_1 - r_2) = \frac{1}{A}\sum_q V_q e^{iq\cdot(r_1-r_2)}. \tag{S6}$$

where r_1 and r_2 above are understood to be operators. Using Eq. (S4) we decompose the position of each particle as:

$$r_1 \equiv R_1 - l^2\epsilon p_1 = R_1 - l^2\epsilon Q_1^T S_1^{-1}\pi_1, \tag{S7}$$

where we are using matrix notation for the two component levi-civita symbol ϵ. We have a similar expression for r_2. Using this we get:

$$e^{iq\cdot(r_1-r_2)} = e^{iq\cdot(R_1-R_2)}e^{-il^2(q_1\cdot\pi_1 - q_2\cdot\pi_2)},$$
$$q_i = -S_i^{-1}Q_i\epsilon q. \tag{S8}$$

In the above expression the terms containing the operator π_1 produce inter-Landau level mixing and we proceed by projecting them into the zeroth landau level which is defined as $a|0\rangle = 0$. By using Eq. (S3) in combination with the BCH formula one can show that:

$$e^{il^2 q\cdot\pi} = e^{-\frac{l^2|q|^2}{4}} e^{\frac{il}{\sqrt{2}}\mathbf{q}a^\dagger} e^{\frac{il}{\sqrt{2}}\mathbf{q}^* a}, \tag{S9}$$

where $\mathbf{q} = q_x + iq_y$. Then one obtains that the projected Hamiltonian is:

$$V_{12} \equiv P_0 V(r_1 - r_2)P_0 = \frac{1}{A}\sum_q V_q e^{-l^2\frac{|q_1|^2+|q_2|^2}{4}} e^{iq\cdot(R_1-R_2)}. \tag{S10}$$

Notice that $q_{1,2}$ are linear functions of q described in Eq. (S8).

For higher Landau levels we need to modify the density form factors. Using Eq. (S9) and the algebra of raising and lowering operators one can show the following identities:

$$\begin{aligned}
&\langle n|e^{il^2 q\cdot\pi}|n\rangle = \\
&= e^{-\frac{l^2|q|^2}{4}}\sum_{m=0}^{n}\left(-\frac{l^2|q|^2}{2}\right)^m \frac{n(n-1)...(n-m+1)}{(m!)^2}, \\
&= e^{-\frac{l^2|q|^2}{4}} L_n\left(\frac{l^2|q|^2}{2}\right),
\end{aligned} \tag{S11}$$

where n is the Landau level of interest and L_n are the Laguerre polynomials. Therefore the interaction projected to the n Landau level is:

$$\begin{aligned}
&v_{12} \equiv P_n v(r_1 - r_2)P_n = \\
&\frac{1}{A}\sum_q v_q L_n\left(\frac{l^2|q_1|^2}{2}\right) L_n\left(\frac{l^2|q_2|^2}{2}\right) e^{-l^2\frac{|q_1|^2+|q_2|^2}{4}} e^{iq\cdot(R_1-R_2)}.
\end{aligned} \tag{S12}$$

III. LANDAU LEVELS AND DENSITY FORM FACTORS FOR ANISOTROPIC DIRAC CONES

The derivation is very similar to that of Galilean electrons. We start from an anisotropic Dirac Hamiltonian:

$$H = \sigma_a g_{ab} p_b = v\sigma'_a\pi_a. \tag{S13}$$

where g is a 3×2 tensor to which we apply a singular value decomposition of the form $g = R^T S Q$, where $R \in SO(3)$ describes a rotation of Pauli matrices σ_a in pseudospin space, $Q \in SO(2)$ describes the transformation of the principal axes in real space, and S is a 3×2 matrix whose upper 2×2 block is diagonal and characterizes the anisotropy of velocities $S = \mathrm{diag}\{(v_x/v_y)^{1/2}, (v_y/v_x)^{1/2}\}$, and whose lower row has zero entries, and $v = (v_x v_y)^{1/2}$. Using the same definition of ladder operators as in Eq. (S3), the Hamiltonian and the spectrum are:

$$\begin{aligned}
&H = \frac{\sqrt{2}v}{l}\begin{pmatrix} 0 & a^\dagger \\ a & 0\end{pmatrix},\ |n,k,s\rangle_D = \frac{1}{\sqrt{2}}\begin{pmatrix} s|n-1,k\rangle \\ |n,k\rangle\end{pmatrix},\ \text{for } n>0 \\
&|0,k\rangle_D = \begin{pmatrix} 0 \\ |0,k\rangle\end{pmatrix},\ E_{nks} = s\frac{\sqrt{2}nv}{l}
\end{aligned} \tag{S14}$$

where $s = \pm$ labels negative and positive energy Landau levels and k is the guiding center intra-Landau level index. From these expressions we can obtain the form factors of the interaction projected to the Dirac Landau levels. One can show that the zero Landau level is identical to the Galilean case, and for the excited Landau levels one gets the same expressions discussed in the previous section but with the modification:

$$L_n\left(\frac{l^2|q|^2}{2}\right) \to \frac{1}{2}\left(L_n\left(\frac{l^2|q|^2}{2}\right) + L_{n-1}\left(\frac{l^2|q|^2}{2}\right)\right) \tag{S15}$$

IV. LANDAU LEVELS AND DENSITY FORM FACTORS IN TILTED DIRAC CONES

To the Hamiltonian, H, appearing in Eqs. (S13), (S14) we add a perturbation describing the tilt of the Dirac cone along the x-direction:

$$H_1 = \delta v_x \pi_x = \delta v_x\sqrt{\frac{v_x}{v_y}}(a + a^\dagger), \tag{S16}$$

where a is defined in Eq. (S3). The (un-normalized) perturbed zero energy Landau level to first order in δv_x is found to be:

$$|0\rangle_1 = \begin{pmatrix} |0\rangle \\ \tau|0\rangle \end{pmatrix}, \tag{S17}$$

where $\tau = \delta v_x/(\sqrt{2}v_y)$. This verifies that the zero Landau level does not carry dipole as expected since particle-hole times inversion is a symmetry. Generically the n-th Landau level will break inversion symmetry however. The valence and conduction first Landau levels have a perturbed form:

$$|\pm 1\rangle_1 = \frac{1}{\sqrt{2}}\begin{pmatrix} |1\rangle \pm \tau(\frac{1}{\sqrt{2}}|2\rangle - |0\rangle) \\ \pm|0\rangle + \tau|1\rangle \end{pmatrix}. \tag{S18}$$

As described in the main text we imagine now two Dirac valleys at opposite momenta and with tilts δv_x of opposite sign and equal magnitude. Let us assume we are filling only one of the two first Landau levels. The form factor obtained from the above perturbative expression is:

$$F_\tau(q) \equiv {}_1\langle 1|e^{il^2 q\cdot\pi'}|1\rangle_1 = \frac{e^{-l^2|q|^2/4}}{Z_\tau}\Big[(1+\tau^2)(1-\frac{q^2}{4})+ \frac{\tau^2}{4}f_{22}(q) + \frac{\tau}{2\sqrt{2}}(f_{12}(q)+f_{21}(q))\Big]. \tag{S19}$$

where $f_{nm}(q) \equiv e^{-l^2|q|^2/4}\langle n|e^{il^2 q\cdot\pi'}|m\rangle$, and Z_τ is the normalization factor of the perturbed states in Eq. (S18). To leading order in τ we can write the form factor as:

$$F_\tau(q) \approx e^{-l^2|q|^2/4}(1-\frac{q^2}{4})(1+\frac{i\tau q_x}{\sqrt{2}}). \tag{S20}$$

One valley will have a form factor corresponding to τ and the other corresponding to $-\tau$ since the tilts have opposite signs. We label them by $\alpha = \{+,-\}$. If one performs the calculation of the exchange energy with these form factors then one finds that the exchange integrals in Eq. (S25):

$$X_{\alpha\beta} = \frac{1}{2}\int \frac{d^2q}{(2\pi)^2} v_q F_\alpha(\bar{q})F_\beta(\bar{q}),\ \bar{q} = -S^{-1}Q\epsilon q. \tag{S21}$$

The exchange energy can then be shown to be:

$$E/N_\phi = \frac{(1-n_z^2)}{2}X_\tau + \text{const.} \tag{S22}$$

with:

$$\begin{aligned} X_\tau =& \frac{X_{++}+X_{--}-X_{+-}+X_{-+}}{2} \\ =& \frac{\tau^2}{2}\int \frac{d^2q}{(2\pi)^2} v_q e^{-l^2|\bar{q}|^2/4}\left(1-\frac{l^2|\bar{q}|^2}{4}\right)^2 l^2\bar{q}_x^2 \end{aligned} \tag{S23}$$

Clearly for a repulsive interaction with $v_q > 0$ we get that X_τ is strictly positive. Therefore the ground state is the Ising nematic ferroelectric state: $n_z = \pm 1$.

V. HARTREE-FOCK THEORY FOR MULTIPLE VALLEYS

We assume the magnetic field is large enough so that the Hamiltonian can be projected into a set of M nearly degenerate Landau levels levels associated with different valleys. The system is at some partial integer filling $\nu \in \mathbb{Z}$ ($\nu \leq M$). We restrict to translationally invariant trial Slater determinant states that are otherwise arbitrary coherent combinations of the M valleys:

$$|\Psi\rangle = \prod_{a=1}^{\nu}\prod_{k=1}^{N_\phi}\left(\sum_{i=1}^{M}\langle\chi_a|i\rangle c_{ki}^\dagger\right)|\text{O}\rangle, \tag{S24}$$

where $|\text{O}\rangle$ is the reference vacuum in which the Landau levels of interest are empty, k is an intra Landau level label, i labels the M valleys, $|\chi_a\rangle$ are N orthonormal vectors describing the occupied coherent combinations of the valleys. The expectation value of the energy (including the neutralizing background) is:

$$\begin{aligned} &E[P] = -N_\phi\sum_{i,j}X_{ij}\langle i|P|j\rangle\langle j|P|i\rangle, \\ &P = \sum_{a=1}^{\nu}|\chi_a\rangle\langle\chi_a|,\ X_{ij} = \frac{1}{2}\int\frac{d^2q}{(2\pi)^2}v_q F_i(q)F_j(-q). \end{aligned} \tag{S25}$$

The solution to the Hartree-Fock problem corresponds to finding the minimum of E with respect to variations of the projector P. One case in which the integrals can be performed analytically is the case in which the interaction correspond to delta-functions in real space, so that $v_q = g$. In this case we have:

$$X_{ij} = \frac{g}{2\pi\sqrt{\text{Det}(1+S_i Q_i Q_j^T S_j^{-2} Q_j Q_i^T S_i)}}. \tag{S26}$$

The behavior of the exchange integrals as a function of valley anisotropy and relative orientation is depicted in Figs. S1-S10. The behavior of higher Landau levels and the Dirac case is qualitatively different but qualitatively similar to the $n = 0$ Landau level as depicted in Figs. S1- S10.

A. Two components at $\nu = 1$

In this case the projector is $P = |\chi\rangle\langle\chi|$, and the exchange energy is:

$$E = -N_\phi\sum_{ij}X_{ij}p_i p_j,\ p_i = |\langle i|\chi\rangle|^2. \tag{S27}$$

The minimization is performed under the constraints $\sum_i p_i = 1$, $p_i \in [0,1]$. We restrict to the case when the two mass tensors have the same eigenvalues but different orientations. Then the Hartree-Fock energy becomes:

$$\frac{E}{N_\phi} = -2(X_{11} - X_{12})(p_1^2 - p_1) - X_{11}, \tag{S28}$$

In Figs. S1- S10 we verify explicitly that in all cases $X_{11} \geq X_{12} \geq 0$. Therefore the energy has minima at $p_1 = \{0, 1\}$ under the constraints in question. Namely the ground state spontaneously chooses one flavor and no coherent combinations and it is spontaneously nematic.

B. three-fold symmetric three-components at $\nu = 1$

Consider now the case of three-components with anisotropic mass tensors oriented in a symmetric three-fold fashion with relative angles $2\pi/3$. In this case the Hartree-Fock energy is:

$$\frac{E}{N_\phi} = -p^T X p, \; X = \begin{pmatrix} X_{11} & X_{12} & X_{12} \\ X_{12} & X_{11} & X_{12} \\ X_{12} & X_{12} & X_{11} \end{pmatrix}. \tag{S29}$$

X has the following eigenvalue decomposition:

$$\begin{aligned} X &= (X_{11} + 2X_{12}) p_0 p_0^T + (X_{11} - X_{12})(\mathbb{I} - p_0 p_0^T), \\ p_0 &= \frac{1}{\sqrt{3}} \begin{pmatrix} 1 \\ 1 \\ 1 \end{pmatrix}. \end{aligned} \tag{S30}$$

Because $X_{11} \geq X_{12} \geq 0$ all the eigenvalues are positive. This implies that the minimum of the energy in Eq. (S29) corresponds to the spontaneously chosen nematics, namely $p_1 = 1$, and $p_2 = p_3 = 0$, and symmetry related copies. The case of $\nu = 2$ is equivalent after performing a particle-hole transformation.

C. four-fold symmetric four-components at $\nu = 1$

This case is special as the ground state is not necessarily nematic but indeed there is a degenerate manifold. We consider four-components with mass tensors oriented in a symmetric four-fold fashion with relative angles $\pi/2$ between adjacent pockets. In this case the Hartree-Fock energy is:

$$\frac{E}{N_\phi} = -p^T X p, \; X = \begin{pmatrix} X_{11} & X_{12} & X_{11} & X_{12} \\ X_{12} & X_{11} & X_{12} & X_{11} \\ X_{11} & X_{12} & X_{11} & X_{12} \\ X_{12} & X_{11} & X_{12} & X_{11} \end{pmatrix}. \tag{S31}$$

The spectrum of X is:

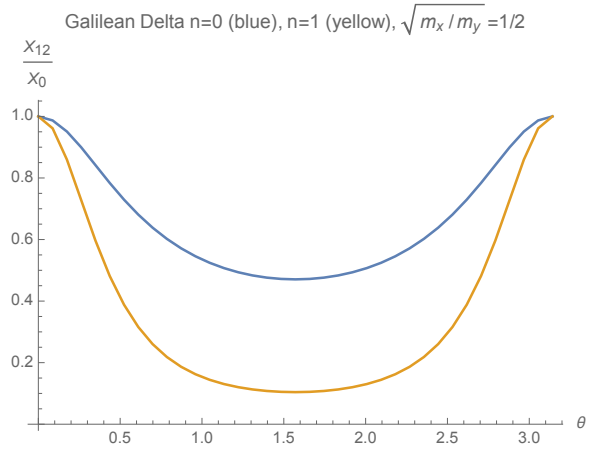

FIG. S1: Comparison between the zero and first Landau level of Galilean case for delta function interactions.

$$\begin{aligned} p_1 &= \frac{1}{\sqrt{2}} \begin{pmatrix} 0 \\ 1 \\ 0 \\ -1 \end{pmatrix}, \; p_2 = \frac{1}{\sqrt{2}} \begin{pmatrix} 1 \\ 0 \\ -1 \\ 0 \end{pmatrix}, \; \lambda_1 = \lambda_2 = 0, \\ p_3 &= \frac{1}{2} \begin{pmatrix} 1 \\ -1 \\ 1 \\ -1 \end{pmatrix}, \; \lambda_3 = 2(X_{11} - X_{12}), \\ p_4 &= \frac{1}{2} \begin{pmatrix} 1 \\ 1 \\ 1 \\ 1 \end{pmatrix}, \; \lambda_3 = 2(X_{11} + X_{12}). \end{aligned} \tag{S32}$$

the structure of eigenvalues implies that minimum will correspond to making $|p_1 + p_3 - p_2 - p_4|$ as large as possible while satisfying the constraints $\sum_\alpha p_\alpha = 1$, $p_\alpha \in [0, 1]$. The solutions are $p_1 + p_3 = 1$, and $p_2 + p_4 = 0$, and symmetry related copies. Notice that CDW type solutions, $p_1 = p_3 = 1/2$, are degenerate with the pure nematic solution in this case, and there is indeed an $SU(2)$ degeneracy remaining that would need to be split by interactions beyond Coulomb.

VI. PROOF OF FULL VALLEY POLARIZATION FOR TWO ANISOTROPIC VALLEYS AT $\nu = 1$ WITHIN HARTREE-FOCK

Consider the situation of two anisotropic valleys labeled $1, 2$. Assume the valleys are related by a discrete rotation by some angle α. This implies that the Landau level have the same energies in both valleys and the eigenstates are related by a discrete symmetry $|2, n, k\rangle = R_\alpha |1, n, k\rangle$, where k is an intra-Landau label for the guiding center degrees of freedom and n is a label for the Landau level of interest. Assume we are at partial filling $\nu = 1$ of any of the doubly degenerate Landau levels of interests. From our general Hartree-Fock expression in Eq. (S25) we obtain that the variational energy is:

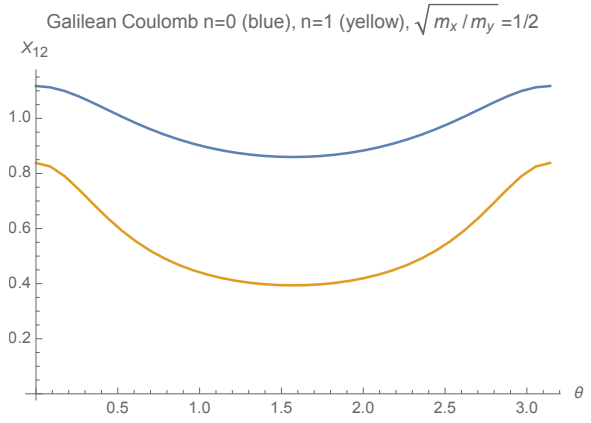

FIG. S2: Comparison between the zero and first Landau level of Galilean case for Coulomb interactions.

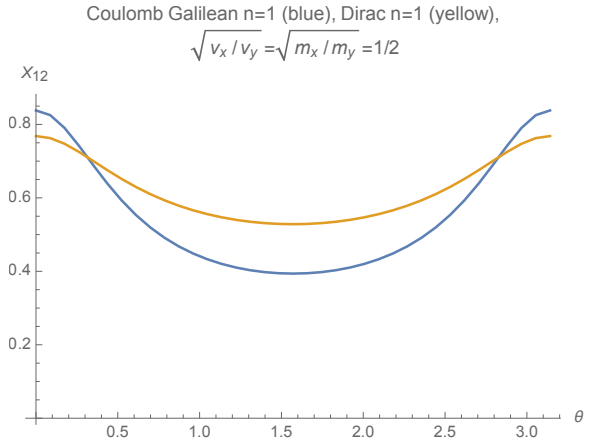

FIG. S3: Comparison of Dirac and Galilean case in the second Landau level for Coulomb interactions.

$$\frac{E}{N_\phi} = -(X_{11}p_1^2 + X_{22}p_2^2 + p_1p_2(X_{12}+X_{21})),\ p_i = |\langle\chi|i\rangle|^2, \quad \text{(S33)}$$

where $|\chi\rangle$ is the vector describing the coherent combination of the two valleys in the valley Bloch sphere and $|i\rangle$ are the vectors corresponding to the two poles of the Bloch sphere. The probabilities are normalized $p_1 + p_2 = 1$. The explicit form of the exchange integrals is:

$$X_{ij} = \frac{1}{2}\int \frac{d^2q}{(2\pi)^2} v_q F_i(q) F_j(-q) \quad \text{(S34)}$$

And the explicit form of the form factors is:

$$F_i(q) \equiv \langle i, n|e^{-il^2 q_a \epsilon_{ab} p_b}|i, n\rangle. \quad \text{(S35)}$$

Because the valleys are related by a rotation R_α by angle α, we have that that $F_2(q) = F_1(R_\alpha^{-1}q)$. This, together with the fact that v_q only depends on the norm $|q|$, implies that $X_{11} = X_{22}$, $X_{12} = X_{21}$ and that these exchange integrals are real numbers. Using this, we can rewrite the energy as:

$$\frac{E}{N_\phi} = -2(X_{11} - X_{12})(p_1 - 1/2)^2 - \frac{X_{11}+X_{12}}{2}. \quad \text{(S36)}$$

The above expression implies that the ground state either spontaneously polarizes into a single valley (Ising type) for $X_{11} > X_{12}$, or into an equal superposition of both valleys (XY type) for $X_{11} < X_{12}$. The marginal case for $X_{11} = X_{12}$ will have effectively SU(2) symmetry and can be an arbitrary coherent superposition of the two valleys.

The form factor satisfies $F_i(q) = F_i(-q)^*$. Interestingly, this implies that the exchange integral can be seen as an inner product in the space of form factors:

$$(F_i, F_j) \equiv X_{ij} = \frac{1}{2}\int \frac{d^2q}{(2\pi)^2} v_q F_i(q) F_j(q)^*. \quad \text{(S37)}$$

It is easy to verify that (F_i, F_j) satisfies all the axioms of an inner product provided v_q is strictly positive (as it is the case for the Coulomb potential) and it is finite because the form factors always have exponential decay as $|q| \to \infty$. Using the Cauchy-Schwarz inequality we can establish that:

$$(F_1, F_2) \leq \sqrt{(F_1, F_1)(F_2, F_2)} \to X_{12} \leq X_{11} \quad \text{(S38)}$$

Therefore we establish that the system generically is of the Ising type and polarizes into a single valley. The inequality is saturated for the marginal case in which $X_{12} = X_{11}$. This happens if and only if the form factor for each valley is separately invariant under the R_α rotation, so that $F_1 = F_2$. This can only happen if the Hamiltonian describing each valley is invariant under the rotation R_α that relates both valleys up to a coordinate independent unitary transformation.

Notice that the above argument implies that if we have two valleys at $\mathbf{k}$ and $-\mathbf{k}$ that are related by a π rotation, but each of the the fermi surfaces of a given valley is not invariant under a π rotation, then the system will polarize into a single valley implying the ground state breaks inversion symmetry and it is a ferroelectric.

VII. PROOF OF FULL VALLEY POLARIZATION FOR MULTIPLE VALLEYS AT $\nu = 1$ WITHIN HARTREE-FOCK

Consider the general case in which we have n valleys located at different regions of momentum space. We do not assume that the valleys are related by symmetry, but only that the form factors are linearly independent functions of $\mathbf{q}$, in the sense implied by the inner product defined by the exchange integral in Eq. (S38). Because the form factors are functions of a two-dimensional wavevector $\mathbf{q}$, we expect that cases in which the form factors are linearly dependent are either fine tuned accidental cases or cases in which a symmetry that relates two

valleys is also a symmetry of the fermi surface within the valley, like the case in which the valleys at opposite momenta have fermi surfaces of identical geometry leading to the SU(2) symmetry case in the two component case described above. In particular, for multi-valley systems in which the valleys are related by a C_n discrete rotational symmetry (rotation by multiples of $2\pi/n$) and the fermi surface of each valley is not individually invariant under any of these discrete rotations, we expect the form factors to be linearly independent. This situation includes the cases of primary interest in our study.

The general expression for the exchange energy is:

$$E = -N_\phi \sum_{ij} X_{ij} p_i p_j, \;\; p_i = |\langle i|\chi\rangle|^2. \tag{S39}$$

Where $|\chi\rangle$ is the trial coherent combination of the valleys labeled by i. The task is to find the minimum of this expression as a function of probabilities p_i that define a point in $\mathbb{R}^n$ that is further restricted to a region defined by the constraints $\sum_i p_i = 1$, $p_i \in [0, 1]$. From the discussion in the previous section it follows that X_{ij} is a real symmetric matrix whose entries are the inner products of vectors in the Hilbert space of form factors: $X_{ij} = (F_i, F_j)$. These matrices are known in linear algebra as Gram matrices and a classic theorem establishes that the linear independence of these vectors implies that the Gram matrix is strictly positive definite implying that all its eigenvalues are real and positive. Now, since X_{ij} is strictly positive definite, it defines itself an inner product in $\mathbb{R}^n$:

$$\mathbf{p}_1 \cdot \mathbf{p}_2 \equiv \sum_{ij} p_{1i} X_{ij} p_{2j}. \tag{S40}$$

Now consider a line in $\mathbb{R}^n$ parametrized by $t \in [0, 1]$ that joins two distinct points, $\mathbf{p}_1$ and $\mathbf{p}_2$, and is described by $\mathbf{p}(t) = t\mathbf{p}_1 + (1-t)\mathbf{p}_2$. Notice that:

$$\|\mathbf{p}(t)\|^2 \equiv \mathbf{p}(t)\cdot\mathbf{p}(t) = \|\mathbf{p}_1 - \mathbf{p}_2\|^2 t^2 + 2t(\mathbf{p}_1\cdot\mathbf{p}_2 - \|\mathbf{p}_2\|^2) + \|\mathbf{p}_2\|^2. \tag{S41}$$

Since the coefficient of the t^2 is strictly positive (because $\mathbf{p}_1 \neq \mathbf{p}_2$) the following statement follows trivially: the maximum of $\|\mathbf{p}(t)\|^2$ is always achieved at the end points of the line and *never strictly within its interior*.

Now, we are considering points within a subset of $\mathbb{R}^n$ defined by the constraints $\sum_i p_i = 1$, $p_i \in [0, 1]$, let us call this region $\mathbf{P}$. $\mathbf{P}$ is contained within a hyperplane in $\mathbb{R}^n$. Now, it is trivial to show that if $\mathbf{p}_1 \in \mathbf{P}$ and $\mathbf{p}_2 \in \mathbf{P}$ then the line that joins them is also contained in this region: $\mathbf{p}(t) \in \mathbf{P}$. Since the energy is $E = -N_\phi \|\mathbf{p}\|^2$, it follows that any point that can be viewed as being *strictly in the interior* of a line contained in $\mathbf{P}$ cannot be a minimum of the energy. Therefore the minima of the energy must be located at the corners of $\mathbf{P}$, because these are the only points which cannot be viewed as being *strictly in the interior* of a line contained within $\mathbf{P}$. The j-th corner is defined by $p_j = 1$ and $p_i = 0$ for $i \neq j$. The state with the minimum energy is therefore fully valley polarized and the valley with minimum energy will be the one with the largest exchange integral X_{jj}. In the case in which the valleys are related by a discrete C_n symmetry the exchange integral X_{jj} will be the same for every j and we get a discrete degeneracy of all the fully polarized states, implying that the system spontaneously fully polarizes into a single valley. For specific examples illustrating this behavior and cases where symmetries allow for X_{ij} to have zero eigenvalues see Section V.

VIII. BERRY PHASE AND POSITION SHIFT FORMULAE OF THE ELECTRIC DIPOLE MOMENT IN A LANDAU LEVEL

To compute the dipole moment along a given direction using the formalism of the modern theory of polarization [4, 5] one choses a gauge so that there is translational invariance along such direction. For example, to compute the dipole along the y direction, we choose $A_x = 0$ and $A_y = Bx$. In this case the single particle states within the Landau level of interest can be labeled by a momentum k_y and have a real space form $\psi_{k_y}(x, y) = \frac{e^{ik_y y}}{\sqrt{L_y}} u_{k_y}(x)$. The problem for the single Landau level becomes quasi-one-dimensional and, for the tilted Dirac cone, we have an effective Hamiltonian:

$$H_{k_y} = \pm(v_x\sigma_x + \delta v_x)(-i\partial_x) + v_y\sigma_y(k_y - eBx). \tag{S42}$$

Translational invariance along the y direction imposes a discretization of $\Delta k_y = 2\pi/L_y$ and periodicity along the x direction determines the size of the effective the Brillouin zone to be: $k_y \in [0, L_x/l^2]$. To determine the polarization we compute the integral over time of the current operator $I_y = -|e|\frac{\partial H_{k_y}}{\partial k_y}$ in response to an adiabatically changing Dirac cone tilt $\delta v_x(t)$ over a period of time T, so that $\delta v_x(t = 0) = 0$ and $\delta v_x(t = T) = \delta v_x$. Following the arguments of Refs. 4, 5, one finds the following expression for the change in the dipole moment per particle:

$$D_y = -i|e|\frac{l^2}{L_x}\int_0^{L_x/l^2} dk_y \langle u_{k_y}|\partial_{k_y}|u_{k_y}\rangle. \tag{S43}$$

In the present case, the real space wave-functions at different k_y differ by a translation: $u_{k_y}(x) = u(x - k_y l^2)$. As a consequence the formula reduces to:

$$D_y = -i|e|\langle u_{k_y}|\partial_{k_y}|u_{k_y}\rangle|_{k_y=0} = i|e|l^2\int dx\, u^*(x)\partial_x u(x). \tag{S44}$$

Using Eq. (S18) and the following expressions for the Landau gauge wavefunctions of Galiliean electrons:

$$\begin{aligned} u_0(x) &= \frac{1}{\pi^{1/4} l^{1/2}} e^{-\frac{x^2}{2l^2}},\; u_1(x) = \frac{i\sqrt{2}x}{\pi^{1/4} l^{1/2}} e^{-\frac{x^2}{2l^2}}, \\ u_2(x) &= \frac{(1-2x^2)}{\sqrt{2}\pi^{1/4} l^{1/2}} e^{-\frac{x^2}{2l^2}}. \end{aligned} \tag{S45}$$

For simplicity assuming $v_x = v_y = v$ one obtains a dipole moment:

$$D_y = \mp |e| l \frac{\delta v_x}{v} \left(1 - \frac{1}{2\sqrt{2}}\right) \tag{S46}$$

Alternatively Eq. (S44) can be cast as follows:

$$\begin{aligned} D_y &= i|e|l^2 \int d^2r\, \psi^*_{k_y}(x,y)\partial_x \psi_{k_y}(x,y) = |e|l^2 \langle \psi_{k_y}|p_x|\psi_{k_y}\rangle \\ &= -|e|\langle \psi_{k_y}|(y - R_y)|\psi_{k_y}\rangle. \end{aligned} \tag{S47}$$

The last expression makes manifest that the dipole moment computed in this way coincides simply with the average position of the single particle orbital measured with respect to the guiding center R_y, which can be thought of as an intra-Landau-level adiabatic invariant that remains constant during the deformation of the wave-function by the tilt of the Dirac cone. The last two equalities are valid in any gauge and can be easily evaluated using the expression of p_x in terms of cyclotron energy raising and lowering operators. In this way we computed the Dipole moment reported in the main text, which agrees with Eq. (S46) in the special case of $v_x = v_y = v$ that we have described here.

IX. WKB EXPRESSION FOR THE DIPOLE MOMENT

Consider a valley with an anisotropic dispersion described by a Hamiltonian $H(p_x, p_y)$. For simplicity we will imagine that the eigenstates near this valley have no Berry phase, or equivalently that the Hamiltonian has only differential operators but no pseudo-spin matrix structure. In the presence of a perpendicular magnetic field, by choosing the Landau gauge $A_x = 0$ and $A_y = Bx$, we can view the eigenvalue problem as effectively one-dimensional, by writing the wavefunction as $\psi_{k_y}(x,y) = \frac{e^{ik_y y}}{\sqrt{L_y}} u_{k_y}(x)$. The eigenstates satisfy:

$$H\left(\frac{\hbar}{i}\frac{d}{dx}, k_y - eBx\right) u_{k_y}(x) = \epsilon u_{k_y}(x) \tag{S48}$$

without loss of generality we set $k_y = 0$, since other solutions are obtained by a global translation. We can search for an approximate WKB solution to this differential equation which formally is an expansion in $\hbar$:

$$u_0(x) = \exp\left(\frac{i}{\hbar}\phi_0(x) + \phi_1(x) + O(\hbar)\right), \tag{S49}$$

substituting this expression into Eq. (S48) and keeping corrections up to linear order in $\hbar$ leads to the WKB form for the solution of the problem:

$$u_0(x) \approx \sum_s \frac{1}{\sqrt{v^{\rm cl}_{x,s}(x,\epsilon)}} \exp\left(\frac{i}{\hbar}\int^x dx' p^{\rm cl}_{x,s}(x',\epsilon)\right), \tag{S50}$$

where $p^{\rm cl}_{x,s}(x',\epsilon)$ is the s root of the algebraic equation defined by the classical dispersion relation: $H(p^{\rm cl}_{x,s}, -eBx) = \epsilon$, and $v^{\rm cl}_{x,s}(x,\epsilon) = \frac{\partial H(p_x,-eBx)}{\partial p_x}|_{p_x \to p^{\rm cl}_{x,s}(x,\epsilon)}$ is group velocity evaluated in the classical trajectory. Typically we have two roots $s = +,-$ and two turning points $x_{+,-}$ that separate the classically allowed region from the classically forbidden region where $p^{\rm cl}_{x,s}$ is imaginary and the wavefunction decays exponentially. As is well known, the quantization condition for the WKB solution is obtained by matching boundary conditions between classically allowed and forbidden regions and leads to the Onsager quantization condition, which, in the absence of Berry phase, reduces to:

$$\sum_s \frac{s}{eB}\int_{p_y^-}^{p_y^+} dp_y p^{\rm cl}_{x,s}(p_y,\epsilon) = l^2 A(\epsilon) = 2\pi(n + 1/2). \tag{S51}$$

where we made the change of variables $p_y = -eBx$, $A(\epsilon)$ is the area in momentum space inside the iso-energetic contour $H(k_x, k_y) = \epsilon$ and n is the Landau level index. From Eq. (S44) we write the Dipole as $D_y = -el^2 \int dx\, {\rm Im}(u^*(x)\partial_x u(x))$. There will be two types of contributions to the dipole moment. One will come from the crossed terms between the two different roots. The semiclassical approximation is expected to work when the oscillations of the wavefunction occur over a length much smaller over that in which the confining potential changes, therefore we restrict to states that have a high energy and hence a large Landau level index. For these states the crossed terms have rapid oscillatory factors of the form $\exp\left(i/\hbar \int^x dx'(p^{\rm cl}_{x,1} - p^{\rm cl}_{x,2})\right)$ and can be neglected. In addition in this case the integrals can be approximated to be taken over the classically allowed region, because the states with rapid oscillations in the classically allowed region correspondingly have fast decay in the classically forbidden region. Therefore the terms in which the oscillatory part cancels within the classically allowed region have the dominant contribution. As a consquence we obtain:

$$\begin{aligned} &\int dx\, {\rm Im}(u^*(x)\partial_x u(x)) \approx \\ &-\sum_s \frac{s}{eB}\int_{p_y^-}^{p_y^+} dp_y \frac{1}{|v^{\rm cl}_{x,s}(p_y,\epsilon)|} p^{\rm cl}_{x,s}(p_y,\epsilon) = -\oint dt\, p_x(t,\epsilon). \end{aligned} \tag{S52}$$

where in the last line we have established the connection to the classical cyclotron motion described in the previous section, in which $d\mathbf{r}(t)/dt = \mathbf{v} = l^2 d\mathbf{k}(t)/dt \times \hat{z}$, from which we have that $v_x = l^2 dp_y/dt$. Additionally we must normalize the WKB solution. Using the same approximations employed to compute the dipole one obtains that the approximate normalization of the WKB solution is:

$$\int dx\, u^*(x)u(x) \approx \sum_s \frac{1}{eB}\int_{p_y^-}^{p_y^+} dp_y \frac{1}{|v^{\rm cl}_{x,s}(p_y,\epsilon)|} = \oint dt. \tag{S53}$$

Thus the normalization is simply the total time that takes to complete the classical cyclotron orbit. A similar analysis can be followed to find the dipole along the x direction D_x. Therefore within the approximations here outlined, the WKB quantized wave-function predicts that dipole moment is simply given by time averaged position of the electron over the semiclassical orbit:

$$\mathbf{D} \approx -|e|\langle \mathbf{r}(t,\epsilon)\rangle_t \equiv -|e|\frac{\oint dt\, \mathbf{r}(t,\epsilon)}{\oint dt}. \tag{S54}$$

where $\mathbf{r}(t,\epsilon)$ is the classical cyclotron orbit determined by the conditions $H(k_x,k_y)=\epsilon$ and $\mathbf{r}(t)=l^2\mathbf{k}(t)\times\hat{z}$, and the speed at which the orbit is traversed is $\mathbf{v}=d\mathbf{r}/dt=\partial H/\partial\mathbf{k}$.

X. SEMICLASSICAL PICTURE OF THE CYCLOTRON MOTION IN TILTED DIRAC CONES

In the semiclassical picture of the cyclotron motion we imagine that both the momentum and the position of the orbit can be simultaneously specified $(\mathbf{r},\mathbf{k})$. The orbit in momentum space, $\mathbf{k}(t)$, is an iso-energetic contour $\epsilon(\mathbf{k}(t))=\epsilon_0$, where $\epsilon(\mathbf{k})$ is energy the dispersion [6]. For simplicity consider a tilted Dirac cone described by a Hamiltonian of the form:

$$H=(v\sigma_x+\delta v_x)k_x+v\sigma_y k_y. \tag{S55}$$

The iso-energy contours in the case of the tilted Dirac cone are off-centered ellipses [7], which by choosing polar coordinates in momentum space (k,θ), read as:

$$k(\theta)=\frac{\epsilon_0}{v+\delta v_x\cos\theta}. \tag{S56}$$

Therefore for $\delta v_x>0$ the ellipse is closest to the origin at $\theta=0$ and farthest at $\theta=\pi$. The real space orbit, however, is a rotated version of the iso-energetic contour: $\mathbf{r}(t)=\mathbf{R}_0+l^2\mathbf{k}(t)\times\hat{z}$, where $\mathbf{R}_0$ is the guiding center. Since the guiding center can be viewed as an adiabatic invariant, this picture explains why upon tilting the Dirac cone, the average position of the orbit relative to its guiding center, $\mathbf{r}(t)-\mathbf{R}_0$, is perpendicular to the direction in which the orbit is tilted in momentum space. This explains intuitively the direction of the dipole we have found in the full quantum calculation. This picture can be further elaborated by considering the speed at which the orbit is traversed. In fact, to leading order in the Dirac cone tilt, the speed at which the semiclassical orbit is traversed is:

$$v=|\partial\epsilon/\partial\mathbf{k}|\approx v+\delta v_x\cos\theta. \tag{S57}$$

Therefore we see that, for $\delta v_x>0$, the speed is such that $v(\theta=0)>v(\theta=\pi)$. This means that the electron moves faster when it is closer to the origin and moves the slowest when it is farther, which further supports the intuition that even in a time averaged sense the momentum of the orbit is shifted towards the direction in which the ellipse is tilted, namely $\langle k_x\rangle<0$, and by symmetry $\langle k_y\rangle=0$. Thus the displacement of the real space orbit is $\mathrm{sign}(B)\langle y\rangle>0$, $\langle x\rangle=0$, explaining the orthogonality of the dipole with respect to the Dirac cone tilt.

XI. DMRG IMPLEMENTATION

Numerically, we consider N electrons moving the surface of torus with a magnetic field perpendicular to its surface. L_x (L_y) represents the circumference of the torus along x (y) direction and they satisfy the relation $L_xL_y=2\pi N_\phi$, where N_ϕ represents the number of orbitals. Here, we set the magnetic length $l_B\equiv\sqrt{\hbar c/eB}$ as the unit of length. In the numerical simulation in this paper, the aspect ratio is set to be 1, i.e., $L_x=L_y$, with angle $\pi/2$. Periodic boundary condition requires $k_y\equiv 2\pi j/L_y$ with $j=0,1,...,N_\phi-1$. The Coulomb interaction on finite size system has the form

$$V(\mathbf{r})=\frac{1}{L_xL_y}\sum_{\mathbf{q}}V(q)\exp(i\mathbf{q}\mathbf{r}) \tag{S58}$$

with $V(q)=2\pi e^2/L_xL_y\varepsilon q$, and the wave-vectors are chosen to guarantee the periodicity of the interaction $V(x+L_x,y)=V\left(x,y+L_y\right)=V(x,y)$. The projected Coulomb interaction between particles i, j into the Lowest Landau level of a valley with mass anisotropic dispersion has the form:

$$V\left(\mathbf{R}_i-\mathbf{R}_j\right)=\sum_{\mathbf{q}}V(q)e^{-q_1^2/2}e^{i\mathbf{q}(\mathbf{R}_i-\mathbf{R}_j)}, \tag{S59}$$

where q_1 is a linear functions of q controlled by the anisotropic mass tensors described in the text immediately following Eq.(10) of the main text and discussed in detailed in Section II below. The matrix elements take the explicit form,

$$V_{j_1j_2j_3j_4}=\delta'_{j_1+j_2,j_3+j_4}\frac{1}{2L_xL_y}\times \sum_{\mathbf{q},\mathbf{q}\neq 0}\delta'_{j_1-j_4,q_yL_y/2\pi}\frac{2\pi e^2}{\varepsilon q}\exp\left[-q_1^2/2-i(j_1-j_3)q_xL_x/N_\phi\right]. \tag{S60}$$

Here, the Kronecker delta with the prime means that the equation is defined modulo N_ϕ. We also consider a uniform and positive background charge so that the Coulomb interaction at $q=0$ are canceled out[1].

For the case of two anisotropic valleys, the Coulomb interaction includes both the intra-component and inter-component interactions. In general, the Coulomb interaction of the two-component systems in the presence of strong magnetic field, after projected onto the lowest Landau level, is written by

$$\begin{aligned}V=&\sum_{i<j}\sum_{\mathbf{q}}V(q)e^{-q_1^2/2}e^{i\mathbf{q}(\mathbf{R}_{1,i}-\mathbf{R}_{1,j})}\\&+\sum_{i<j}\sum_{\mathbf{q}}V(q)e^{-q_2^2/2}e^{i\mathbf{q}(\mathbf{R}_{2,i}-\mathbf{R}_{2,j})}\\&+\sum_{i<j}\sum_{\mathbf{q}}V(q)e^{-(q_1^2+q_2^2)/4}e^{i\mathbf{q}(\mathbf{R}_{1,i}-\mathbf{R}_{2,j})}.\end{aligned} \tag{S61}$$

Here, the first two terms are intra-component Coulomb interaction, and the last term is inter-component Coulomb interaction, and $q_{1,2}$ are the linear functions of q controlled by the anisotropic mass tensors of each valley described in the text immediately following Eq.(10) of the main text and in Section II below. A similar expression to Eq. (S61) holds for the explicit matrix elements.

Simulations are realized by mapping the single particle orbitals into one dimensional lattice. The advantage of the density matrix renormalization group (DMRG) method, compared to exact diagonalization, is that it can achieve reliable results for larger system sizes. In this manuscript, we impose momentum-space DMRG method on torus, where each site in x direction corresponds to different states labeled by the momentum in y direction. The standard procedure is similar to real-space DMRG, but since the non-zero Coulomb interaction exists between the orbitals satisfying the momentum conservation $j_1 + j_2 = j_3 + j_4$ mod N_ϕ, only small number of momentum sectors in each DMRG block contributes to the ground state in the initial process. To ensure the convergence, one has to save more momentum sectors with keeping a small number of states in these sectors during the initial process, which may become important in the later DMRG sweep, while the remaining states are selected following the standard DMRG algorithm to reach the required truncation accuracy. For our calculation, we keep around $2000 \sim 8000$ states and perform measurement during each DMRG sweep until the data is converged.

We study N electrons in two-components and each component has $N_\phi = N$ orbitals. We found that in the ground state the charge distributes uniformly into the two orbitals for isotropic case [8], i.e., $m_x/m_y = 1$, while the ground state is realized in a sector in which all electrons polarize into a single orbital with the same flavor for anisotropic case, as shown in the Fig. S4 for $N = N_\phi = 24$ system with $(m_x/m_y)^{1/4} = 1.5, 2$.

To study charged excitations we search for ground states with one particle added to those described above. The behavior of the charged excitations is markedly distinct for large and small anisotropic ratio m_x/m_y. When the anisotropic ratio is large enough, as shown in Fig. S5 for $N = N_\phi + 1 = 21$ system with $(m_x/m_y)^{1/4} = 2$, N_ϕ electrons will fully occupy the orbitals with the same flavor, while the extra one will stay at the orbital with another flavor. The position of this extra electron is determined by the total momentum $K/(2\pi/N_\phi)$ targeted in DMRG simulation, but different momentum sectors have the same energy due to translational invariance. This is consistent with the behavior of the conventional quasiparticle predicted by Hartree-Fock analysis. However, for smaller m_x/m_y ratio, as shown in Fig. S6 with $(m_x/m_y)^{1/4} = 1.2$, the total number of electrons in the majority flavor will be smaller than N_ϕ, while he number of particles in the minority flavor will be larger than one, indicating that the quasiparticle has a nontrivial pseudo-spin texture. Here, the electron number depends on both anisotropic ratio m_x/m_y and system size N. Fig. S7 shows the finite size scaling of the charge gap in the quasiparticle regime. We calculate the charge gap Δ_{gap} for the systems with $N_\phi = 12$ to $N_\phi = 28$ and the anisotropic ratio $(m_x/m_y)^{1/4} = 1.6$ and $(m_x/m_y)^{1/4} = 1.8$. We fit the data as a quadratic function of $1/N_\phi$, and estimate the thermodynamic limit of the gap by extrapolating $1/N_\phi \to 0$.

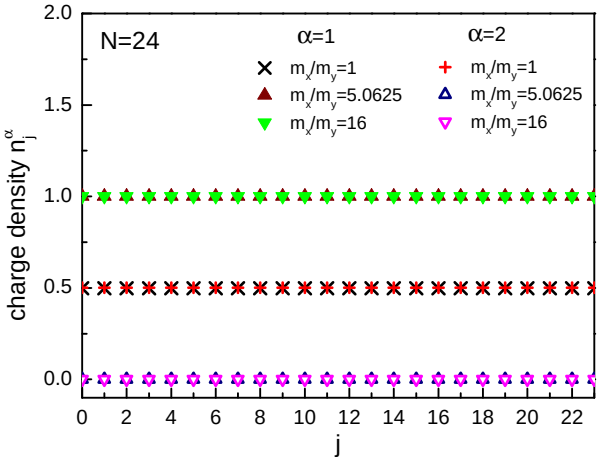

Fig. S4: The charge density distribution for $N = 24$ ($N_\phi = N$) system with anisotropic ratio $m_x/m_y = 1, 5.0625, 16$. All of electrons tend to stay in the same flavor α orbitals ($j = 0, 2, \ldots, N_\phi - 1$) for anisotropic case. $\alpha = 1, 2$ represent two components.

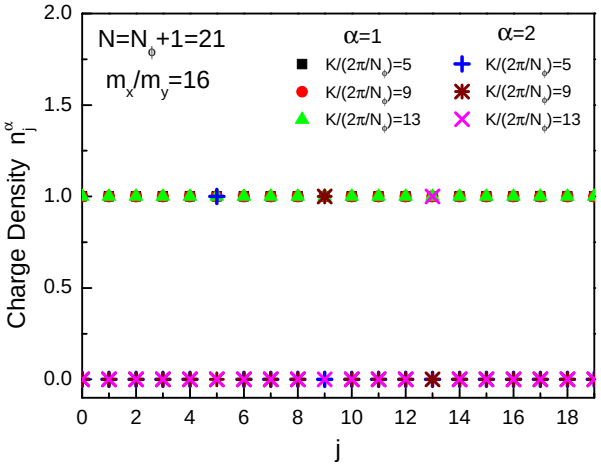

Fig. S5: The charge density distribution for $N = 21$ ($N_\phi = 20$) system with anisotropic ratio $m_x/m_y = 16$. The extra electron will stay in the orbital $K/(2\pi/N_\phi)$ if one target the corresponding total momentum, and the ground state energies are the same for different targeting momentum sectors.The total electron number for two flavors are $N_1 = 20$ and $N_2 = 1$.

XII. COMPARISON BETWEEN HARTREE-FOCK AND DMRG QUASIPARTICLE GAP

The charge gap in Hartree-Fock theory can be shown to coincide with minus twice the energy per particle of the ground

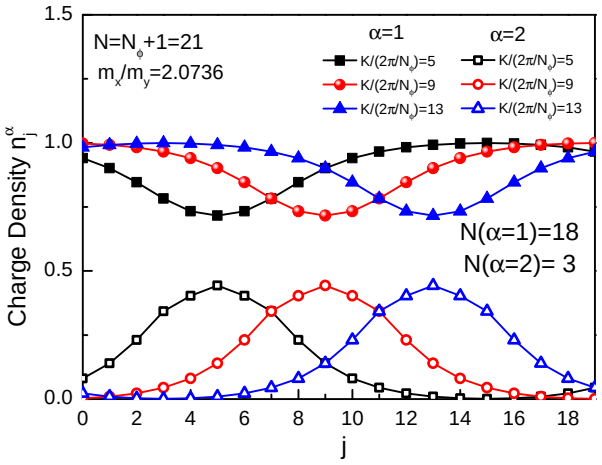

Fig. S6: The charge density distribution for $N = 21$ ($N_\phi = 20$) system with anisotropic ratio $m_x/m_y = 2.0736$. The extra electron will stay near the orbital $K/(2\pi/N_\phi)$ if one target the corresponding total momentum, and the ground state energies are the same for different targeting momentum sectors. The electron number for two flavors are $N_1 = 18$ and $N_2 = 3$, which depends on the system size.

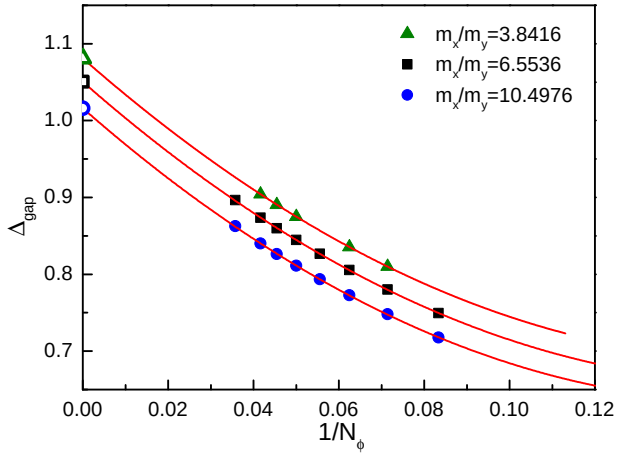

Fig. S7: The finite size scaling of charge gap at quasiparticle regime for $m_x/m_y = 6.5536$ and $m_x/m_y = 10.4976$. The system size ranges from $N_\phi = 12$ to $N_\phi = 28$.

state, which, for the Coulomb interaction, can be found to be:

$$\Delta^{HF}_{\text{charge}} = -2\frac{E^0_{HF}}{N_\phi} = \frac{K(1-m_y/m_x)}{(m_x/m_y)^{1/4}}\sqrt{\frac{2}{\pi}}\frac{e^2}{l}. \tag{S62}$$

Here E^0_{HF} is the Hartree-Fock energy of the ground state with no quasiparticles and K is the elliptic integral of the first kind. This formula corrects a typo in Ref. 2. Figure S8 illustrates the Hartree-Fock charge gap for the conventional quasi-electron and quasi-hole pair computed within Hartree-Fock theory and compared to the results from DMRG. After extrapolation to

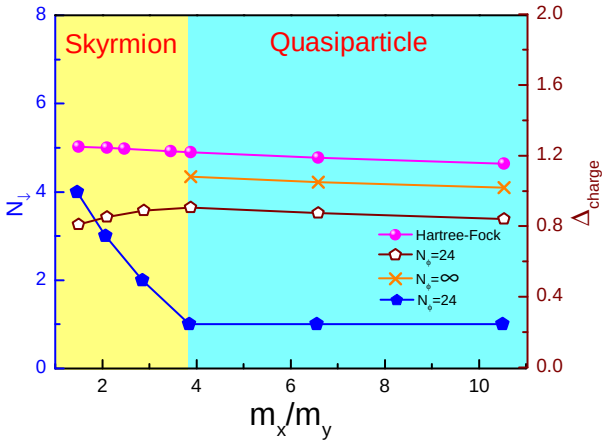

FIG. S8: The left vertical axis shows the number of spin flips (blue) involved in the lowest energy charged quasiparticle as a function of mass anisotropy for a system with two anisotropic pockets like AlAs. The right vertical axis shows different calculations of the charge gap including Hartree-Fock (purple) and DMRG for the largest system size (white) and the extrapolated values to infinite size (yellow).

infinite sizes the results show good agreement in the large mass anisotropy regime where quasi-particles are no longer expected to be skyrmions.

The physical reason for the decreasing gap at large anisotropies is that as the anisotropy increases the overlap between orbitals becomes smaller and their exchange energy gain is reduced. Because the energy gain per particle is reduced it is also less energetically costly to add or remove particles, making the gap a decreasing function of mass anisotropy.

XIII. ISING SKYRMIONS FROM NON-LINEAR SIGMA MODEL

Starting from Eq. (S28) we can write $p_1 \equiv \frac{n_z+1}{2}$, where $n_z \in [-1, 1]$ is the z-component of the Ising pseudospin. Then the energy of a non-linear sigma model with this anisotropy can be written as (up to a global constant) [2]:

$$\begin{aligned} E &= \int d^2r \frac{\rho_s}{2}|\nabla n|^2 + \frac{\alpha}{2}(1-n_z^2), \\ \alpha &= \frac{X_{11}-X_{12}}{2\pi l^2}, \end{aligned} \tag{S63}$$

and we have neglected the anisotropy of the stiffness. Because the stiffness term is scale invariant, this model alone is unable to determine the optimal size of the Skyrmions. In addition it is necessary to include the Coulomb energy associated with the Skyrmion charge [3]:

$$\begin{aligned} E_c &= \frac{e^2}{2}\int d^2r d^2r' \frac{\rho(r)\rho(r')}{|r-r'|}, \\ \rho(r) &= \frac{1}{8\pi} n(r)\cdot[\partial_x n(r)\times\partial_y n(r)]. \end{aligned} \tag{S64}$$

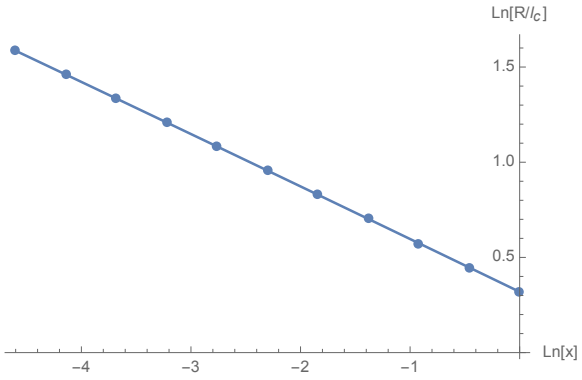

FIG. S9: Log-Log plot illustrates power law approximates well the skyrmion size as a function of dimensionless Ising anisotropy $x = \alpha l_c^2/\rho_s$.

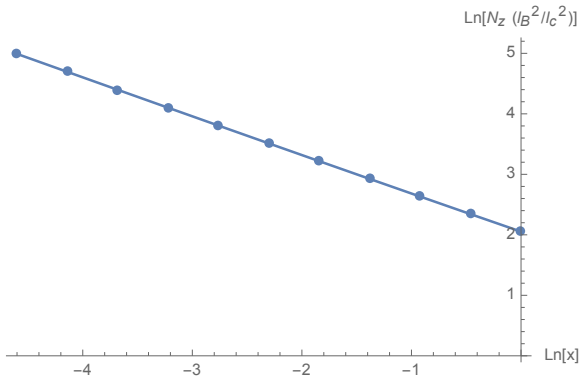

FIG. S10: Log-Log plot of the number of spin flips involved in the Skyrmion, N_z, as a function of dimensionless Ising anisotropy $x = \alpha l_c^2/\rho_s$.

There are two length scales in the problem:

$$\begin{aligned} l_c &\equiv \frac{e^2}{16\pi^2\rho_s} \approx \frac{\sqrt{2}}{\pi^{3/2}} l_B \\ \lambda &\equiv \sqrt{\frac{\rho_s}{\alpha}}. \end{aligned} \tag{S65}$$

The length scale l_c essentially is the magnetic length, l_B, if one uses the value for the stiffness from the isotropic limit $\rho = \frac{e^2}{16\sqrt{2}\pi l_B}$. λ is the typical size of the Ising domain wall in the limit in which one neglects Coulomb energies. Let us define the dimensionless ratio:

$$x = \frac{\alpha l_c^2}{\rho_s} = \frac{l_c^2}{\lambda^2}. \tag{S66}$$

The minimal energy Skyrmion will carry charge one and is rotationally invariant for the case of isotropic stiffness. We performed numerical minimization of the energy functional under these approximations. Defining the Skrymion radius as $n_z(R_{Skyr}) = 0$, we found that the following power law fits well the results:

$$\begin{aligned} R_{Skyr} &= \frac{C_R}{x_R^\beta} l_c, \\ C_R &\approx 1.4,\ \beta_R \approx 0.27 \pm 0.05. \end{aligned} \tag{S67}$$

Similarly, taking the boundary condition $n_z(r \to 0) = 1$ and $n_z(r \to \infty) = -1$, we can define the spin of the Skyrmion (number of spin-flips relative to the ground state) as:

$$N_z = \frac{1}{2\pi l_B^2} \int d^2 r \frac{n_z(r) + 1}{2}. \tag{S68}$$

Then we find the following power law fits well the numerical results depicted in Fig.

$$\begin{aligned} N_z &\approx \frac{l_c^2}{l_B^2} \frac{C_z}{x^{\beta_z}}, \\ C_z &\approx 1.4,\ \beta_z \approx 0.3. \end{aligned} \tag{S69}$$

For small mass anisotropy we can approximate $\alpha \approx \frac{3\Delta_0}{32(2\pi l_B^2)}(s-1)^2$, with $s^2 \equiv \frac{m_>}{m_<}$, which leads $x \approx \frac{3(s-1)^2}{4\pi^3}$. Using this approximation and the numerical solution, one can estimate that the critical mass anisotropy for the system to have the smallest non-trivial Skyrmion (with $N_z > 2$) is:

$$x_{crit} \approx 0.00004,\ s_{crit}^2 \approx 1.08. \tag{S70}$$

This tiny amount of anisotropy is already enough to shrink skyrmions to be usual spin flip Hartree-Fock quasiparticles. As discussed in the main text we find however we find that the critical mass ratio is about $s_{crit}^2 \approx 3.8$, highlighting the inadequacy of combining the long wavelength parameters for this non-linear sigma model in order to estimate small skyrmions.

XIV. SIMPLIFIED CALCULATION OF CHARGE GAP FROM PARTICLE-HOLE SYMMETRY

The chemical potential is the energy change for adding a particle. Thus the chemical potential to add a quasi-electron on top of the Ising magnet is:

$$\mu_+ = E_{N=N_\phi+1} - E_{N=N_\phi}. \tag{S71}$$

Similarly the chemical potential for quasiholes is:

$$\mu_- = E_{N=N_\phi} - E_{N=N_\phi-1}. \tag{S72}$$

The charge gap is defined as the jump in chemical potential:

$$\Delta_{charge} = \mu_+ - \mu_- = E_{N=N_\phi+1} + E_{N=N_\phi-1} - 2E_{N=N_\phi}. \quad \text{(S73)}$$

We now use particle hole symmetry which is present in our problem. Under particle-hole the Hamiltonian transforms as:

$$\mathcal{C}\mathcal{T}H\mathcal{C}\mathcal{T}^{-1} = H + 2E_{N=N_\phi}\left(1 - \frac{N}{N_\phi}\right). \quad \text{(S74)}$$

from this it can be established that:

$$E_{N=N_\phi-1} = E_{N=N_\phi+1} - 2\frac{E_{N=N_\phi}}{N_\phi}. \quad \text{(S75)}$$

And that the charge gap has the following form:

$$\Delta_{charge} = 2\left(E_{N=N_\phi+1} - E_{N=N_\phi}\left(1 + \frac{1}{N_\phi}\right)\right). \quad \text{(S76)}$$

[S1] Daijiro Yoshioka, Phys. Rev. B 29, 6833(1984).

[S2] D. A. Abanin, S. A. Parameswaran, S. A. Kivelson, and S. L. Sondhi, Phys. Rev. B **82**, 035428 (2010); A. Kumar, S. A. Parameswaran, and S. L. Sondhi Phys. Rev. B 88, 045133 (2013).

[S3] M. Abolfath, J. J. Palacios, H. A. Fertig, S. M. Girvin, and A. H. MacDonald, Phys. Rev. B **56**, 6795 (1997).

[S4] D. J. Thouless, Phys. Rev. B **27**, 6083 (1983).

[S5] R. D. King-Smith and D. Vanderbilt, Phys. Rev. B **47**, 1651(R) (1993).

[S6] C. Kittel, Introduction to solid state, John Wiley & Sons, (1966).

[S7] I. Sodemann and L. Fu, Phys. Rev. Lett. **115**, 216806 (2015).

[S8] The method selects a single sector even in this case in which there are SU(2) related degenerate copies.